Graefes Arch Clin Exp Ophthalmol (2010) 248:435–441
DOI 10.1007/s00417-009-1259-3

GLAUCOMA

Linear discriminant analysis and artificial neural network for glaucoma diagnosis using scanning laser polarimetry–variable cornea compensation measurements in Taiwan Chinese population

Mei-Ling Huang · Hsin-Yi Chen · Wei-Cheng Huang · Yi-Yu Tsai

Received: 22 June 2009 / Revised: 10 November 2009 / Accepted: 19 November 2009 / Published online: 15 December 2009

Abstract
Background To determine whether linear discriminant analysis (LDA) and artificial neural network (ANN) can improve the differentiation between glaucomatous and normal eyes in a Taiwan Chinese population, based on the retinal nerve fiber layer thickness measurement data from scanning laser polarimetry–variable corneal compensation (GDx VCC).
Methods This study comprised 79 glaucoma (visual field defect, mean deviation: −5.60±4.23 dB) and 86 healthy subjects (visual field defect, mean deviation: −1.44±1.72 dB). Each patient received complete ophthalmological evaluation, standard automated perimetry (SAP), and GDx VCC exam. One eye per subject was considered for further analysis. The area under the receiver operating characteristics (AROC) curve, sensitivity, specificity and the best cut-off value for each parameter were calculated. The diagnostic performance of artificial neural network (ANN) and linear discriminant analysis (LDA) for glaucoma detection using GDx VCC measurements will be compared in this study.
Results The individual parameter with the best AROC curve for differentiating between normal and glaucomatous eye was nerve fiber indicator (NFI, 0.932). The highest AROCs for the LDA and ANN methods were 0.950 and 0.970 respectively.
Conclusion NFI, ANN and LDF method demonstrated equal diagnostic power in glaucoma detection in a Taiwan Chinese population.

Keywords Linear discriminant analysis · Artificial neural network · Scanning laser polarimetry–variable cornea compensation · Glaucoma diagnosis

Presented in part at: Asia ARVO, March 2007, Singapore and ARVO, May 2007, Fort Lauderdale, Florida, America.

The authors have full control of all primary data, and we agree to allow Graefe's Archive for Clinical and Experimental Ophthalmology to review our data.

Commercial relationships policy: N

M.-L. Huang
Department of Industrial Engineering & Management,
National Chin-Yi University of Technology,
35, Lane 215, Section 1, Chung-Shan Road,
Taiping City, Taichung County 411, Taiwan

H.-Y. Chen (✉) · W.-C. Huang · Y.-Y. Tsai
Department of Ophthalmology,
China Medical University Hospital,
No. 2, Yuh-Der Road,
Taichung City 404, Taiwan
e-mail: hsin7850@url.com.tw

Introduction

Some evidence shows that retinal nerve fiber layer (RNFL) analysis may improve the diagnosis of early glaucomatous damage [21, 24]. Scanning laser polarimetry (SLP) is an imaging modality available for assessing RNFL thickness. The accuracy of SLP in diagnosing glaucoma was limited, because the measurements obtained could be affected by the factor of corneal polarization; therefore, a new model of SLP employs a variable corneal polarization (GDx VCC; Carl Zeiss Meditec, Inc.) compensator that allows for eye-specific compensation [8, 9, 27]. Some studies have shown that GDx VCC demonstrates moderate to good discriminating power for glaucoma detection [2, 3, 6, 18–20, 23]. GDx VCC includes a summary parameter called the nerve

fiber indicator (NFI), which was developed from a machine-learning classifier known as the support vector machine (SVM) [26]. Some studies have reported that NFI has superior diagnostic performance compared with individual parameters [3, 19, 23, 27]. To increase the diagnostic accuracy for glaucoma detection, some analytic tools that use different SLP measurements as input parameters were developed, by using statistical methods such as linear discriminant analysis (LDA) [3, 18]. The LDA method assumes that data representing different groups are linearly separable. If this assumption is not well-met, the classifier's performance is degraded. Furthermore, several machine-learning methods have been proposed to increase the accuracy of diagnosing glaucoma disease [2, 6, 20]. However, different study designs and different ethnic groups have led to conflicting outcomes. Therefore, the aim of this study was to evaluate the accuracy of GDx VCC in glaucoma detection in a Taiwan Chinese population. We apply the parameter selection technique to retrieve GDx-VCC variables for the LDA and ANN analyses. The performance of the LDA and ANN methods for evaluating GDx VCC parameters will be compared based on the AROC curve in the current study.

Subjects and methods

This observational cross-sectional study included one randomly selected eye from each of 165 study participants (79 patients with glaucoma and 86 healthy controls) who had sought treatment at the Department of Ophthalmology, China Medical University Hospital (CMUH). This research follows the tenets of the Declaration of Helsinki. Informed consent was obtained from all participants, and the study was approved by the Institutional Review Board of the CMUH.

Each subject underwent a complete ophthalmic examination, including slit-lamp biomicroscopy, gonioscopy, pachymetry, Goldmann applanation tonometry, stereoscopic examination of the optic disc and fundus, and standard automated perimetry (SAP, 30-2 mode, Humphrey Field Analyzer, model 750, HFA; Carl Zeiss Meditec, Inc.). All subjects underwent GDx VCC imaging within 3 months of the clinical examination and visual field testing. Subjects with a best-corrected visual acuity of less than 20/40, a spherical equivalent outside ±5.0 diopters, and a cylinder correction >3.0 diopters were excluded. Patients with eyes with coexisting retinal disease, uveitis, or nonglaucomatous optic neuropathy were also excluded from this study.

Normal control eyes had normal findings in clinical examination, intraocular pressures (IOP) of 21 mm Hg or less with no history of increased IOP, normal-looking optic nerve [14] (intact rim, no evidence of hemorrhage, focal rim thinning , notching, glaucomatous excavation or RNFL defects) and a normal visual field result. A normal visual field was defined as a mean deviation (MD) and pattern SD (PSD) within 95% confidence limits, and a Glaucoma Hemifield Test (GHT) result within normal limits.

Eyes were classified as glaucomatous if they had repeatable (two consecutive) abnormal visual field test results, defined as a PSD outside the 95% normal confidence limits, or a GHT result outside 99% normal confidence limits, regardless of the appearance of the optic disc. To avoid bias in the evaluation of the optic disc, the definition of glaucoma was based on the visual field result, which is not dependent on RNFL or optic disc morphology [7].

SLP measurements

SLP measurements were obtained by the same trained and experienced technician. The images were analyzed with software version 5.5.0. The software also provided an image quality check score (1–10) to ensure accurate corneal measurement. In our study, the images had to be of high quality, i.e., a well focused, even, centered optic disc without any motion artifact. In addition, a score of 7 was the minimum standard for imaging quality. The 15 GDx VCC-measured RNFL thickness parameters comprised TSNIT average (total average RNFL thickness), superior average, inferior average, the TSNIT standard deviation, nerve fiber indicator (NFI), symmetry, superior ratio, inferior ratio, superior/nasal, maximum modulation, superior maximum, inferior maximum, ellipse modulation, normalized superior area, and normalized inferior area. All parameters, except for NFI, were used in the LDA and ANN.

Entropy-based feature selection

The traditional definition of entropy refers to changes in the status quo of the system, a measure of "molecular disorder", and the amount of energy wasted in a dynamical energy transformation from one state or form to another [10]. Entropy change has often been defined as a change to a more disordered state at a molecular level [16]. In this study, we removed the irrelevant GDx parameter by calculating the value of entropy. The procedure starts from the complete data set including fourteen GDx-VCC parameters, and the parameter of which the removal most retains the distinctness among the clusters should be removed first. The similarity measure (S) was used to assume a very small value (close to 0.0) for very close pairs of instances, and a very large value (close to 1.0) for very

distant pairs [4]. For a dataset of N instances, the entropy measure is given as:

$$E = -\sum_{i=1}^{N}\sum_{j=1}^{N}\left(S_{ij}\times\log S_{ij} + \left(1-S_{ij}\right)\times\log\left(1-S_{ij}\right)\right) \quad (1)$$

where S_{ij} is the similarity value, normalized to [0,l], between the instances x_i and x_j.

$$S_{ij} = e^{-\alpha\times D_{ij}} \quad (2)$$

where D_{ij} is the distance between the instances x_i and x_j, and α is a parameter.

A sequential backward selection algorithm for unsupervised data (SUD) was used to determine the relative importance of features [4]. We used Matlab software version 6.5 to run the SUD to determine the importance of 14 GDx VCC parameters.

Linear discriminant analysis (LDA)

Linear discriminant analysis (LDA) is a statistic method which can classify objects into two mutually exclusive groups based on the dataset in which researchers are interested. LDA combines input parameters into a discriminant function to classify cases in different groups. The idea underlying this classification method is to develop a linear discriminant function, F, of n variables as $F = \beta_1 x_1 + \beta_2 x_2 + \ldots + \beta_n x_n$ with values for β_1, β_2, ..., β_n chosen so as to maximize the between-group to within-group sum of squares ratio, where the independent variables (x) are the features that can describe the objects; the result represents the best discrimination between the two groups. In this study, we analyzed 14 parameters, obtained from GDx VCC, by LDA, for their ability to differentiate between glaucomatous and healthy eyes. Detailed descriptions of the statistical procedures involved in the assessment and use of LDA models can be found in the literature [15]. SAS software version 10.0 was used for LDA.

Table 1 Demographics of the normal and glaucoma groups

	Normal (n=86)	Glaucoma (n=79)	P-value
Gender			
Male, n (%)	40 (47%)	42 (53%)	0.393
Female, n (%)	46 (53%)	37 (47%)	
Age (years)	40.20±15.54	44.30±14.72	0.083
Pattern standard deviation (dB)	1.95±1.17	5.86±4.89	0.000
Refraction	-2.02±2.23	-2.38±3.15	0.407
Mean deviation (dB)	-1.44±1.72	-5.60±4.23	0.000

* compared by t-test method

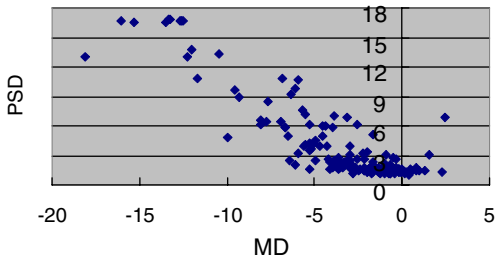

Fig. 1 The scatter plot of MD vs PSD in whole eyes

Artificial neural network (ANN)

An ANN can be structured to perform classification [22], An ANN consists of one input layer, one output layer, and one or more hidden layers that extract essential information during learning. ANNs can mimic the behavior of biological neural nets, and have successfully solved problems through generalization of a limited quantity of training data, overall trends in functional relationships. A well-trained ANN can be used to simulate and predict the output response for various control factor-level settings. In this study, for different inputs of parameter combinations generated from entropy, two to fourteen neurons in

Table 2 GDX- VCC measured RNFL thickness in both groups

	Normal	Glaucoma	P-value
TSNIT average(μm)	59.77±5.33	50.56±8.67	<0.001
Superior average(μm)	72.76±6.39	58.80±10.04	<0.001
Inferior average(μm)	70.81±9.50	56.47±12.09	<0.001
TSNIT SD (μm)	24.33±4.42	19.86±5.98	<0.001
Nerve fiber indicator (NFI)	14.94±6.52	40.91±19.53	<0.001
Symmetry	1.01±0.15	0.99±0.20	0.542
Superior ratio	3.05±1.09	2.28±1.03	<0.001
Inferior ratio	3.06±1.19	2.34±1.01	<0.001
Superior/nasal	3.23±0.80	2.74±0.85	<0.001
Max modulation	2.81±0.98	2.25±1.05	<0.001
Superior maximum(μm)	86.34±10.63	71.76±14.82	<0.001
Inferior maximum(μm)	86.36±11.45	74.35±18.81	<0.001
Ellipse modulation	4.04±1.49	3.71±1.69	0.190
NSA*	0.152±0.0209	0.116±0.0327	<0.001
NIA*	0.154±0.0272	0.117±0.0399	<0.001

NSA: normalized superior area; NIA: normalized inferior area; SD: standard deviation.

*Compared by Student's t-test

Table 3 The AROC, sensitivity & specificity and best cut-off value of each parameter for differentiating normal from glaucomatous eyes

Parameter	Normal vs glaucoma			
	AROC	Sensitivity	Specificity	Best cut-off value
TSNIT average	0.815	62.03	98.84	<51.24
Superior average	0.879	72.15	97.67	<62.99
Inferior average	0.835	67.09	87.21	<62.22
TSNIT SD	0.748	70.89	68.60	<22.3
NFI	0.932	83.54	93.02	>23
Symmetry	0.537	31.65	86.05	<0.88
Superior Ratio	0.734	58.23	84.88	<2.1
Inferior Ratio	0.698	63.29	68.60	<2.39
Superior/Nasal	0.675	63.29	63.95	<2.85
Max Modulation	0.669	43.04	87.21	<1.73
Superior Maximum	0.809	68.35	87.21	<75.01
Inferior Maximum	0.723	59.49	86.05	<75.50
Ellipse Modulation	0.573	29.11	90.70	<2.31
Normalized Sup. Area	0.835	69.62	91.86	<0.1225
Normalized Inf. Area	0.792	55.70	94.19	<0.1224

SD: standard deviation

the ANN hidden layer were executed. The neural network classifier is trained to detect a relationship between input (GDx VCC parameters) and a predefined gold-standard diagnosis by comparing its prediction with the labeled diagnosis, and by learning from its mistakes [25]. Ten-fold cross-validation was applied. The whole dataset was divided into ten sets. Each set contained one tenth of the normal people and one tenth of the glaucoma patients in the original dataset. The first set was treated as a test set; the second set was treated as a validation set, and the remaining eight sets were used as training sets. Each set was iterated as a test set, and the whole procedure was run ten times. Finally, the test results from all eyes were then used to plot the ROC curve. Matlab software version 6.5 was used for ANN application.

Statistical analyses

Statistical analyses were performed on a personal computer using SPSS (Ver.12.0; SPSS, Chicago, IL, USA). Differences in age, visual field mean deviation (MD), and average RNFL thickness measured with GDx VCC between groups were evaluated by the *t*-test. The AROC curve was used to assess the ability of each testing parameter to differentiate between normal and glaucomatous eyes (MedCalc software, version 9.0). In all statistical analyses, we set significance at 0.05/N, where N is the number of tests used (Bonferonni correction). The standard methods of comparing the areas under receiver operating characteristic curves were described by Delong DM et al. [5] and Hanley & McNeil [11]. In this work, pair-wise comparisons of AROC between LDA and ANN, between LDA and NFI, and between ANN and NFI were made by MedCalc software version 9.0 according to the method proposed by Hanley and McNeil [11].

Results

Table 1 shows the demographics of each group. The mean age was 40.20±15.54 years in the control group and 44.30± 14.72 years in the glaucoma group. There was no significant difference in age between the groups (p=0.083). The average MD of visual field was −1.44±1.72 dB in the control group

Table 4 Entropy values by removing one parameter from the entire data set

Order	1	2	3	4	5	6	7
Attribute	Superior maximum	Inferior maximum	Inferior average	Superior average	TSNIT SD	TSNIT average	Ellipse modulation
Entropy	98.01	97.6	77.09	72.56	58.83	55.94	47.44
Order	8	9	10	11	12	13	14
Attribute	inferior ratio	superior ratio	max modulation	superior/nasal	symmetry	normalized inf. area	normalized sup. area
Entropy	46.66	46.62	46.24	46.05	45.25	45.24	45.24

Table 5 The AROCs of LDA with different number of parameters as LDA input

Number of variables	AROC	Number of variables	AROC
1	0.809	8	0.948
2	0.809	9	0.949
3	0.895	10	0.948
4	0.922	11	0.948
5	0.922	12	0.947
6	0.928	13	0.949
7	0.930	14	0.950

and −5.60±4.23 dB in the glaucoma group. The average PSD of visual field was 1.95±1.17 dB in the control group and 5.86±4.89 dB in the glaucoma group. There were significant differences in MD and PSD values between the control and glaucoma groups ($p<0.05$). To test the feasibility of our study sample, we evaluated the correlation between MD and PSD in each eye as shown in Fig. 1, and the result showed that they were highly correlated. Table 2 lists the GDx VCC data from both groups. There were significant differences in all parameters between control and glaucoma groups, except for the two parameters symmetry and ellipse modulation).

Table 3 lists the AROC for differentiating normal from glaucomatous eyes for each parameter. The parameter with the best AROC curve was NFI (0.932, C.I. 0.882–0.965).

Table 4 shows the entropy values with respect to the situation when one specific parameter was removed from the whole data set. We obtained the order list of variables based on the result of SUD, and the GDx VCC variables were ranked as inputs both for LDA and ANN in the following sequence: inferior maximum, superior maximum, inferior average, superior average, TSNIT SD, TSNIT average, ellipse modulation, inferior ratio, superior ratio, max modulation, superior/nasal, symmetry, normalized inferior area, and normalized superior area.

Table 5 and Fig. 2 show the AROCs for LDA when different numbers of variables were used. The highest AROC (0.950) was achieved when 14 variables were fed as the input dataset for LDA. Figure 3 shows the AROCs for ANN when different numbers of neurons were used. The performance of parameter selection using SUD was very successful; the highest AROC achieved was 0.970 when 11 variables were used as the input dataset.

Figure 4 shows the AROCs curves using the LDA method, ANN method and NFI parameter. The highest AROC with the LDA method is 0.950 (C.I. 0.905 to 0.978); and the highest AROC with the ANN method is 0.970 (C.I. 0.932 to 0.990). The difference between the best ANN and best LDA AROCs was not statistically significant ($p=0.357$); the difference between the best ANN and NFI AROCs was not statistically significant ($p=0.117$); the difference between NFI and the best LDA AROCs was not statistically significant ($p=0.310$).

Discussion

Our study confirms the previous work in which GDx VCC demonstrated a good discriminating power in glaucoma detection [2, 3, 6, 18–20, 23], and we also agree with the concept that NFI is the most important parameter in glaucoma detection. Interestingly, we found that both ANN and LDF methods cannot improve upon standard software-provided GDx VCC measurement, NFI, in glaucoma detection. The value of NFI was generated from an advanced form of neural network analysis. It was trained on a large sample of representative healthy and glaucomatous eyes, and utilized information from the entire RNFL thickness map to optimize the discrimination between the two. In our preliminary report, we found that the LDA method slightly improved the diagnostic capability of glaucoma based on the GDx VCC measured parameters (2007, Huang WC & Chen HY, et al. Asia ARVO E-Abstract

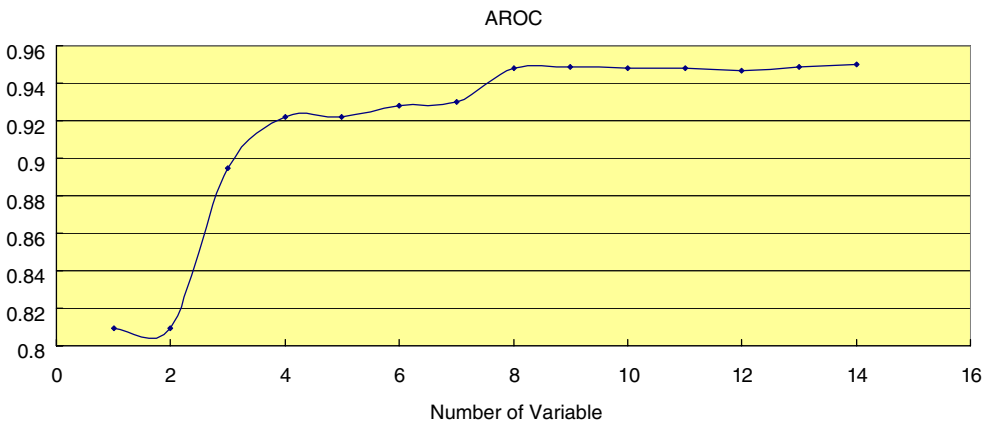

Fig. 2 The AROCs for LDA when different numbers of variables were used

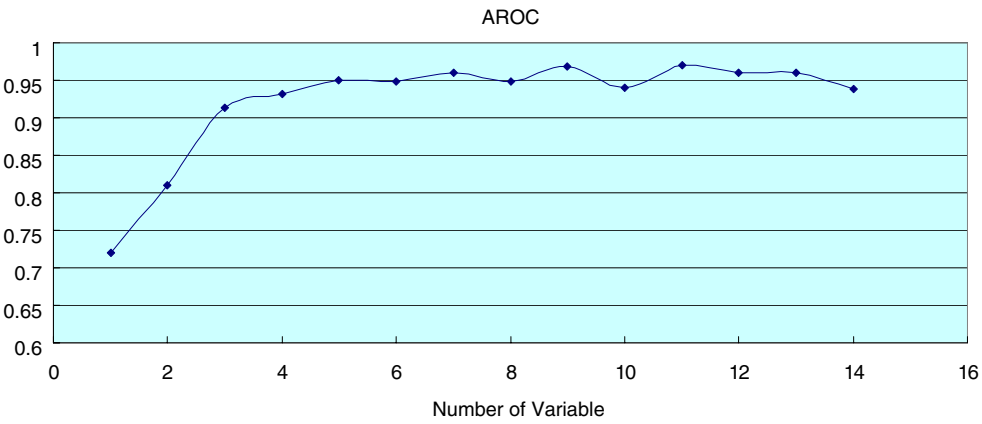

Fig. 3 The AROCs for ANN when different number of neurons were used

307). The parameter with the best AROC curve (glaucoma visual field, average MD, −3.32±2.20 dB) was NFI (0.795). For LDA with stepwise method, the AROC for glaucoma detection was 0.845 with four input parameters (TSNIT average, superior, inferior, and Inferior maximum). In addition, we also reported that the ANN method could improve the diagnostic capability of glaucoma (average MD, −6.83±7.21 dB) based on the GDx VCC-measured parameters (AROC from ANN, 0.984; NFI, 0.82) (2007, Chen HY et al., ARVO E-Abstract 500). Here in the current study, we directly compare the two classification methods in the same study population (glaucoma, visual field severity, MD, −5.60±4.23 dB). The current result suggests that LDA and ANN trained on SLP RNFL thickness measurements are similar, and provide accurate classification of glaucomatous and healthy eyes.

Glaucoma diagnosis based on medical image data is common in medical decision-making. For group classification, LDA is a well-established method for classifying patients into different groups, and is commonly used in glaucoma [1, 12, 13, 28]. The LDA method has also been applied to the Heidelberg Retina Tomograph (HRT) parameters [1] and the Stratus OCT parameters in glaucoma diagnosis [12]. Previously, Weinreb et al. [28] also developed a structural LDA based on SLP readings which could increase the diagnostic ability in glaucoma detection. In this study, we first applied the LDA method to evaluate the GDx VCC database in a pure Chinese population. However, the result shows that the diagnostic performance of the LDA method is no better than the NFI parameter. NFI is developed using a machine-learning classifier, the support vector machine (SVM). SVM is a popular machine classification method that directly minimizes the classification error without requiring a statistical data model. Because of its simple implementation and consistently high classification accuracy, many real-world classification situations have been applied. Bowd C et al. [1] reported that HRT-based neural network techniques performed as well as or better than HRT-based LDFs. We believe that our current study is the first one to directly compare the LDF method with the ANN method in the same population using GDx VCC parameters. And the result also confirms the pervious work of Bowd C et al., although different optical imaging machines were used and a different population was chosen.

Machine-earning methods have recently been applied in the issue of glaucoma diagnosis. Bowd C et al. [2] reported that AROC curves for optimized RVM (0.93) and SVM (0.91) were significantly larger than those for NFI (AROC, 0.87). In our study, the ANN method shows excellent performance in glaucoma detection (AROC, 0.970) in a Taiwan Chinese population. Although the result is promising, it is inadequate for directly comparing the ANN result with that of the NFI, because of the differences in selection criteria for study inclusion.

There are some limitations of our study, although the results are interesting. The primary limitation is that, although the present sample size was adequate, a larger sample size is needed to obtain a standardized classification function. Second, the substrate for studies is usually a

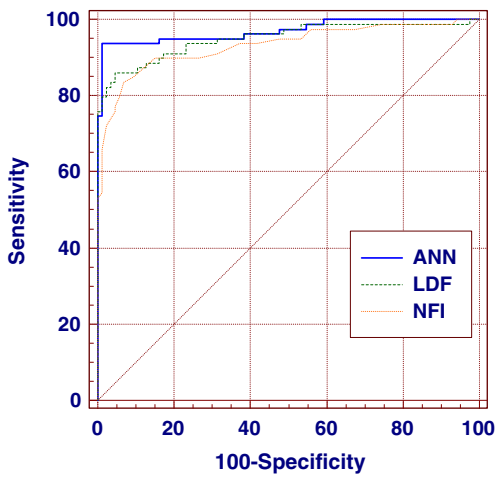

Fig. 4 The AROC curves using the LDA method, ANN method and NFI parameter

clinic-based population of patients with glaucoma. These patients are identified on the basis of particular patterns of structural and functional abnormality which meet preconceived notions that bias the outcome of the comparisons [17]. Moreover, the selection of a high-quality image process might produce some bias. Therefore, there is still some room for improving glaucoma detection using different methods.

Although the results from LDA and ANN trained on GDX VCC measurements are similar, and provide adequate classification between glaucomatous and healthy eyes in Taiwan Chinese population, the machine-learning classifier shows good potential in glaucoma diagnosis.

Acknowledgments The authors would like to thank for the National Science Council of the Republic of China for financially supporting this research under Contract No. 97-2628-E-167-001-MY3& DMR-93-046, DMR-94-043.

References

1. Bowd C, Chan K, Zangwill LM, Goldbaum MH, Lee TW, Sejnowski TJ, Weinreb RN (2002) Comparing neural networks and linear discriminant functions for glaucoma detection using confocal scanning laser ophthalmoscopy of the optic disc. Invest Ophthalmol Vis Sci 43:3444–3454
2. Bowd C, Medeiros FA, Zhang Z, Zangwill LM, Hao J, Lee TW, Sejnowski TJ, Weinreb RN, Goldbaum MH (2005) Relevance vector machine and support vector machine classifier analysis of scanning laser polarimetry retinal nerve fiber layer measurements. Invest Ophthalmol Vis Sci 46:1322–1329
3. Brusini P, Salvetat ML, Parisi L, Zeppieri M, Tosoni C (2005) Discrimination between normal and early glaucomatous eyes with scanning laser polarimeter with fixed and variable corneal compensator settings. Eur J Ophthalmol 15:468–476
4. Dash M, Liu H, Yao J (1997) Dimensionality Reduction of Unsupervised Data. Proceedings of the Ninth IEEE International Conference on Tools with AI (ICTAI'97), Newport Beach, CA, pp 532–539
5. DeLong ER, DeLong DM, Clarke-Pearson DL (1988) Comparing the areas under two or more correlated receiver operating characteristic curves: a nonparametric approach. Biometrics 44:837–845
6. Essock EA, Zheng Y, Gunvant P (2005) Analysis of GDx-VCC polarimetry data by Wavelet-Fourier analysis across glaucoma stages. Invest Ophthalmol Vis Sci 46:2838–2847
7. Garway-Heath D, Hitchings RA (1998) Sources of bias in studies of optic disc and retinal nerve fibre layer morphology. Br J Ophthalmol 82:986
8. Garway-Heath DF, Greaney MJ, Caprioli J (2002) Correction for the erroneous compensation of anterior segment birefringence with the scanning laser polarimeter for glaucoma diagnosis. Invest Ophthalmol Vis Sci 43:1465–1474
9. Greenfield DS, Knighton RW, Feuer W, Schiffman JC, Zangwill L, Weinreb RN (2002) Correction for corneal polarization axis improves the discriminating power of scanning laser polarimetry. Am J Ophthalmol 134:27–33
10. Haddad WM, Chellaboina VS, Nersesov S (2006) Thermodynamics: a dynamical systems approach. IEEE Transactions on Automatic Control 51:1217–1225
11. Hanley JA, McNeil BJ (1983) A method of comparing the areas under receiver operating characteristic curves derived from the same cases. Radiology 148:839–843
12. Huang ML, Chen HY (2005) Development and comparison of automated classifiers for glaucoma diagnosis using stratus optical coherence tomography. Invest Ophthalmol Vis Sci 46:4121–4129
13. Iester M, Jonas JB, Mardin CY, Budde WM (2000) Discrimination analysis models for early detection of glaucomatous optic disc changes. Br J Ophthalmol 84:464–468
14. Jonas JB, Budde WM, Panda-Jonas S (1999) Ophthalmoscopic evaluation of the optic nerve head. Surv Ophthalmol 43:293–320
15. Kleinbaum DG, Kupper LL, Muller KE (1998) Applied regression analysis and other multivariate methods, 2nd edn. PSW-Kent, Boston
16. Lambert FL (2002) A cracked crutch for supporting entropy discussions. J Chem Educ 79:187–192
17. Medeiros FA, Ng D, Zangwill LM, Sample PA, Bowd C, Weinreb RN (2007) The effects of study design and spectrum bias on the evaluation of diagnostic accuracy of confocal scanning laser ophthalmoscopy in glaucoma. Invest Ophthalmol Vis Sci 48:214–222
18. Medeiros FA, Susanna RJ (2003) Comparison of algorithms for detection of localized nerve fiber layer defects using scanning laser polarimetry. Br J Ophthalmol 87:413–419
19. Medeiros FA, Zangwill LM, Bowd C, Mohammadi K, Weinreb RN (2004) Comparison of scanning laser polarimetry using variable corneal compensation and retinal nerve fiber layer photography for detectionof glaucoma. Arch Ophthalmol 122:698–704
20. Poinoosawmy D, Tan JC, Bunce C, Hitchings RA (2001) The ability of the GDx nerve fiber analyzer neural network to diagnose glaucoma. Graefes Arch Clin Exp Ophthalmol 239:122–127
21. Quigley HA, Addicks EM, Green WR (1982) Optic nerve damage in human glaucoma III: quantitative correlation of nerve fiber loss and visual field defect in glaucoma, ischemic neuropathy, apilledema and toxic neuropathy. Arch Ophthalmol 100:135–146
22. Raimundo IM, Narayanaswamy R (2001) Simultaneous determination of relative humidity and ammonia in air employing an optical fibre sensor and artificial neural network. Sens Actuators B 74:60–68
23. Reus NJ, Lemij HG (2004) Diagnostic accuracy of the GDx VCC for glaucoma. Ophthalmology 111:1860–1865
24. Sommer A, Miller NR, Pollack I, Maumenee AE, George T (1977) The nerve fiber layer in the diagnosis of glaucoma. Arch Ophthalmol 95: 2149–2156
25. Tomatis S, Bono A, Bartoli C et al (2003) Automated melanoma detection: multispectral imaging and neural network approach for classification. American Association of Physicists in Medicine 2:212–221
26. Vapnik V (2000) The Nature of Statistical Learning Theory, 2nd edn. Springer, New York
27. Weinreb RN, Bowd C, Zangwill LM (2003) Glaucoma detection using scanning laser polarimetry with variable corneal polarization compensation. Arch Ophthalmol 120:218–224
28. Weinreb RN, Zangwill L, Berry CC, Bathija R, Sample PA (1998) Detection of glaucoma with scanning laser polarimetry. Arch Ophthalmol 116:1583–1619